INFLUENCES OF DIFFUSER VANES PARAMETERS AND IMPELLER MICRO GROOVES DEPTH ON THE VERTICALLY SUSPENDED CENTRIFUGAL PUMP PERFORMANCE

D. Khoeini

Department of Mechanical Engineering,
Isfahan University of Technology,
Isfahan, Iran

E. Shirani

Department of Mechanical Engineering,
Foolad Institute of Technology,
Fooladshahr, Isfahan, Iran

ABSTRACT

Effects of geometric parameters of diffuser vanes as well as impeller micro grooves depth on the performance of a vertically suspended centrifugal pump have been studied. Different diffuser vanes height, leading angles, trailing angles, wrapping angles and furthermore, impeller micro grooves depths have been analyzed thoroughly. Numerical results have been verified by comparing experimental data. Results, without considering cavitation, reveal that diffuser vanes height has the profound impact on the vertically suspended centrifugal pump performance followed by vanes wrapping angle. Additionally, it is observed that delivered head and efficiency of micro-grooved impellers reduce more by flow rate enhancing rather than that of the original impeller.

Keywords: Vertically suspended centrifugal pump; Geometric parameters; Diffuser vanes; Impeller micro grooves; Performance characteristics

1. INTRODUCTION

Vertically suspended centrifugal pumps are regarded as an inevitable part of various industries such as oil and chemical plant industries, desalination industries which are becoming more and more important due to fresh water crisis all around the world (for pumping seawater to associated desalination units) and other aspects accordingly. Hence, in order to approach higher performance they have been investigated [1-10] along with making modification of other types of centrifugal pumps [11-18].

Zhu *et al*. [1] performed a numerical analysis of the rotating impeller of a submersible pump to recognize flow pattern using the transient multiphase Computational Fluid Dynamics (CFD). The k-ε turbulence model was employed in their research. Results revealed that the VOF model is inferior to Eulerian-Eulerian multiphase model for gas-liquid two-phase flow simulation as Eulerian-Eulerian model showed good agreement with experiments. Zhou *et al*. [2] studied diffuser vanes number of a suspended single-stage pump in three different cases of 6, 7, and 8. Computations were carried out based on SST k-ω turbulence model. The increase of pump head was seen with the enhancement of vanes number. However, blockings and more hydraulic losses were reported due to excessive vanes, that obtained under over-loading circumstances. The less hydraulic losses were achieved using seven vanes. Geometric parameters of a vertically suspended pump were surveyed by Ofuch *et al*. [3]. They utilized dimensional analysis as an alternative to investigate performance degradation of pump numerically for a wide range of viscosities (1–810 mm2 /s) and different rotational speeds (1800–3500 rpm). They utilized turbulence model coupled with the Gamma Theta transition model. A correlation for head and flow rate correction factors due to viscosity was accomplished to predict performance degradation. Zhang *et al*. [4] investigated design features of a mixed- flow submersible pump. They found that the axial- radial guide vane has higher performance than the radial guide vane of the tested pump. Two- phase flow through a split vane impeller of a multi- stage submersible pump was surveyed by Pirouzpanah *et al*. [5] using Electrical

* Corresponding author (dkhoeini@gmail.com)

DOI : 10.1017/jmech.2019.13
Copyright © 2019 The Society of Theoretical and Applied Mechanics

https://doi.org/10.1017/jmech.2019.13 Published online by Cambridge University Press

Table 1 Pump parameters

Impeller	Impeller Dia.	550 mm
	Inlet blade angle	17°
	Outlet blade angle	21°
	Number of blades	6
	Blade height	40 mm
	Blade thickness	8 mm
	Rotating speed	1475 rpm
Diffuser	Number of vanes Inlet Dia.	8 560 mm
Micro-grooved Impeller	Number of micro grooves	84
	Width of a micro groove	2 mm
	Depth of a micro groove	0 micron
		300 micron
		900 micron

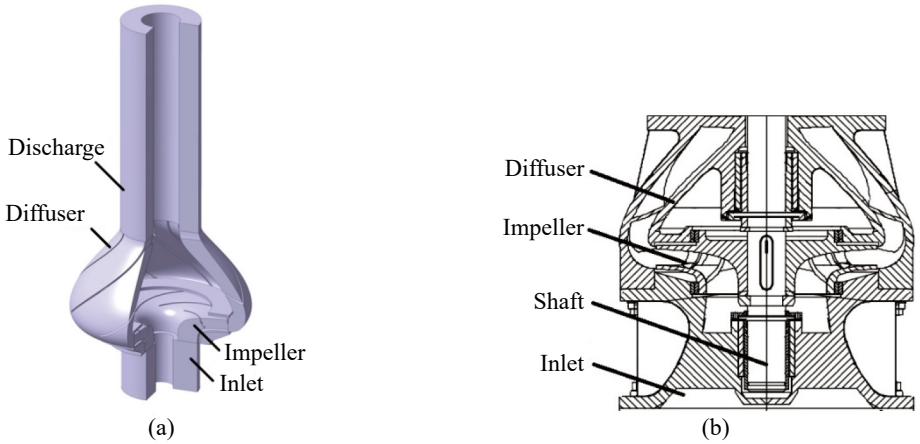


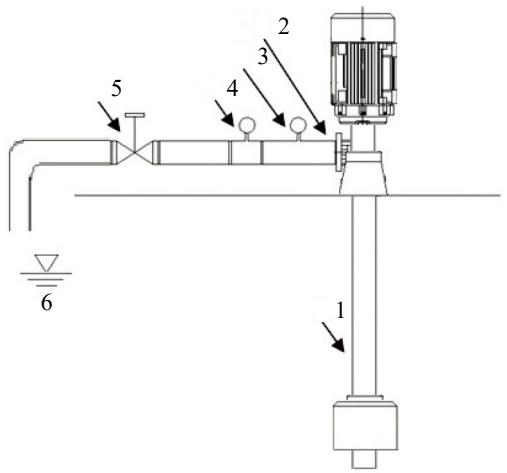
Fig. 1. Vertically suspended centrifugal pump (a) Sectional view of flow domain (b) Manufactured cross-sectional view

Resistance Tomography (ERT) and pressure measurements. Their results showed that the second stage has better performance in comparison with the first stage. Besides, they observed that the rotating speed and inlet pressure have negligible impacts on the head ratio of the third stage of the multi- stage pump. Zhu *et al*. [6] conducted numerical and experimental studies on the effects of oil viscosity on multi- stage submersible pump. By increasing viscosity, some recirculation occurred at blade trailing edges. Also, it is resulted that total pressure dropped remarkably along streamline due to the impeller-diffuser interaction. Pineda *et al*. [7] examined phase distribution of inlet water- air flow in a submersible pump. Results at higher rotation speeds demonstrated higher scatter of void fraction for the pump. Moreover, the head declined with higher gas flow rates as well. Flow characteristics of a submersible multistage pump were measured by Stel *et al*. [8]. In off-design operation a restriction of the stage net outflow area was resulted because of the reverse flow zones in the pump. A deep-well submersible centrifugal pump with different diffusers was researched by Zhou *et al*. [9]. They achieved higher performance by using three- dimensional surface return diffuser rather than the traditional cylindrical return diffuser. Sun and Prado [10] modelled gas- liquid performance of a submersible pump. A new correlation to predict distributions of pressure and void fraction in impeller and diffuser of pump were proposed. Additionally, pump performance with different fluid properties and rotational speeds were analysed as well.

In the part of micro-grooved impeller, a study has been reported recently. Indeed, impeller micro grooves role on the performance of a volute type centrifugal pump having low specific speed (Ns=8) were investigated by Skrzypacz and Bieganowski [11] in two cases of micro-grooved and not micro-grooved impeller. Delivered head and efficiency of micro-grooved impeller were increased compared with not micro-grooved impeller.

Considering previous studies, although some research have been carried out on the performance of vertically suspended centrifugal pumps but the effect of h/H ratio of diffuser vanes (h is the diffuser vane height and H is the height of diffuser passage area) and impeller micro grooves depth of vertically suspended centrifugal pumps have received no attention by the authors. Indeed, no research has

https://doi.org/10.1017/jmech.2019.13 Published online by Cambridge University Press



1. Vertically suspended pump	4. Flow meter
2. Outlet pipe	5. Globe valve
3. Pressure gage	6. Water storage

Fig. 2 Schematic view of test apparatus

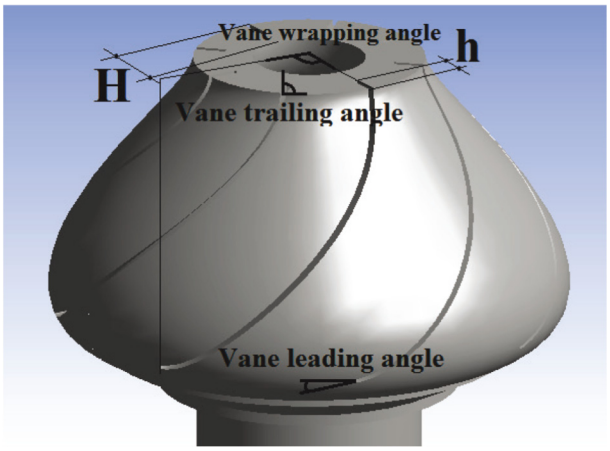


Fig. 3 Computational domain of diffuser with parametric dimensions of vanes

been conducted to investigate the influences of h/H ratio of diffuser vanes and impeller micro grooves depth on the performance of vertically suspended centrifugal pumps, yet. Therefore, in the present research, the impacts of different geometric parameters of diffuser vanes consisting h/H =0.25, 0.5, 0.75 and 1, leading angles of 3, 10 and 17 degree, trailing angles of 70, 90 and 110 degree, wrapping angles of 58, 78 and 98 degree and impeller micro grooves depths (d=0, 300 and 900 micron) on the performance of a vertically suspended centrifugal pump have been studied numerically and the optimum case was then built to perform experiments.

2. DIFFERENT PARTS OF A VERTICALLY SUSPENDED CENTRIFUGAL PUMP

Different parts of the vertically suspended centrifugal pump having specific speed 18.2 including inlet, impeller, diffuser and discharge regions are illustrated in Fig. 1. Indeed, sectional view of flow domain and cross-sectional view of the manufactured pump are shown in Figs. 1 (a) and (b), respectively. Furthermore, all parameters are listed in Table 1 which is composed of inlet and outlet diameters, impeller diameter, impeller blades number, leading and trailing angles of blades, blade thickness and height, etc.

3. TEST APPARATUS

Fig. 2 indicates schematic view of test apparatus. In this investigation, the performance of the aforementioned vertically suspended centrifugal pump has been tested by using water at $25°C$ [19]. At different flow rates all performance curves, head versus flow rate and overall efficiency versus flow rate, have been achieved based on [19-20]. Actually, to this end, an electromagnetic flowmeter has been installed at the discharge pipe to measure different flow rates (Q). In order to control the operation of the pump, a globe valve has been employed at the discharge pipe as well. Discharge pressures have been obtained under each test condition. Moreover, according to [21] values of head and flow rate and absorbed power uncertainties have been resulted ±1.9%, ±2.6%, ±2.1% , respectively. Also, Reynolds Number of the mentioned pump is 55.4*106

4. COMPUTATIONAL ANALYSES

4.1 Geometry

In Fig. 3 computational domain of diffuser with parametric dimensions of vanes have been shown. In separate analyses each diffuser with different vanes characteristics of h/H=0.25, h/H=0.5, h/H=0.75, h/H=1, leading angles of 3, 10 and 17 degree, trailing angles of 70, 90 and 110 degree, wrapping angles of 58, 78 and 98 degree has been studied numerically. Additionally, the impacts of impeller micro grooves depths have been analyzed as well. Next, the optimum case was manufactured for performing experiments.

4.2 Mesh generation

Computational grid for flow domain is demonstrated in Fig. 4. In the proximity of acute regions, grids have been refined. Structured mesh has been used in the vicinity of walls and unstructured mesh has been utilized in other regions.

4.3 Governing equations

In the present research, the incompressible 3-D steady state Navier- Stocks equations [22] have been solved by the commercial CFD software ANSY-CFX:

$$\nabla \boldsymbol{U} = 0 \tag{1}$$

https://doi.org/10.1017/jmech.2019.13 Published online by Cambridge University Press

Table 2 The elements analysis for impeller

Grid size (×1000)	852	1250	1712	2581
Head (m)	48.9	54.6	56.5	57

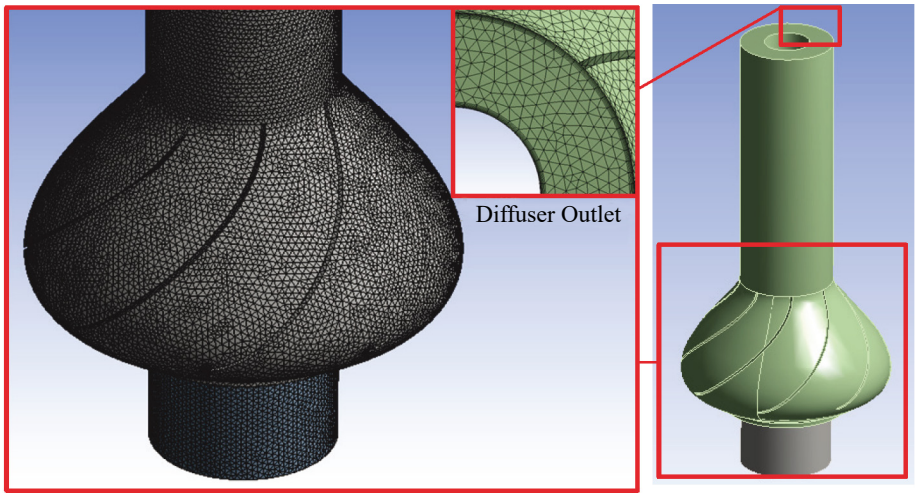


Fig. 4. Computational grid for flow domain

$$\rho\nabla.(\boldsymbol{UU}) = -\nabla p + \nabla.(\tau) + \rho\boldsymbol{g} + \boldsymbol{F} \quad (2)$$

where ρ, U and p, denote the fluid density, absolute velocity and pressure, respectively. Moreover, τ and F present stress tensor and source term. For discretization of diffusion terms, central difference and for convective terms, second order scheme have been used. Besides, SST turbulence model has been employed in this research as the accuracy of SST turbulence model has been validated in various studies [23]. Additionally, approach of frozen rotor has been utilized in all computations as at the aforementioned scheme, the rotational impacts are specified as source term (F) in the equations of momentum. And the rotor is considered as stationary part. The total pressure (approximately 1.2 bar as experiments have been then carried out by submersible depth of 0.2 bar) and uniform flow with turbulent intensity of 1% has been regarded at inlet boundary condition. The boundary condition of mass flow rate (700, 1000, 1300, 1600 and 2000 m3/h) at the outlet boundary and no slip condition at all walls have been specified in numerical analyses. Furthermore, the value of Y+ remained lower than 50 for all cases [24-26]. And also, discretization of mentioned equations have been done using a three-dimension Navior-stokes CFD code (finite volume one) and converging criteria of 10-6 has been considered for all residual figures.

4.4 Grid verification

Table 2 gives results of the head predicted for different grid sizes. To ensure grid dependence a difference of one percent between the two different grid results was considered. Eventually, the grid size of 2581×1000 elements was chosen for computations.

4.5 Comparison of the experimental and numerical results

Actually, a vertically suspended centrifugal pump having specific speed 18.2 has been investigated by making adjustments in diffuser vanes parameters (h/H=0.25, h/H=0.5, h/H=0.75 and h/H=1, leading angles of 3, 10 and 17 degree, trailing angles of 70, 90 and 110 degree, wrapping angles of 58, 78 and 98 degree) and providing micro grooves on the impeller passageways. However, the diffuser vanes are the structural member of the diffuser to support the diffuser hub to the outer diffuser shroud but different h/H ratios have been investigated numerically for analyzing the impacts of diffuser vanes heights. Then, the optimum case was manufactured and experiments have been done.

A comparison between the numerical and experimental results for diffuser with h/H =1 and leading angle of 10 degree, trailing angle of 90 degree and wrapping angle of 78 degree and original impeller (not micro-grooved) is presented in Fig. 5. As depicted, numerical data is consistent with experimental results and the highest discrepancy of 8.3 percent is observed at the same conditions (inlet pressure, working fluid) due to the reason of flow through clearances in experiments.

Furthermore, error bars have been indicated in tested points separately in Fig. 5 based on maximum difference among repeated measurements of the same measure that is 0.9 percent.

5. RESULTS

5.1 Influences of diffuser vanes height

In order to study different aspects of flow fields in the

https://doi.org/10.1017/jmech.2019.13 Published online by Cambridge University Press

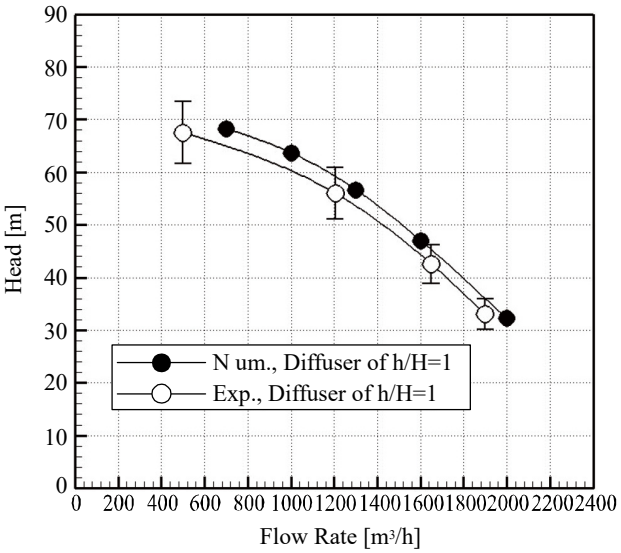


Fig. 5. Head as a function of flow rate, experimental and numerical results

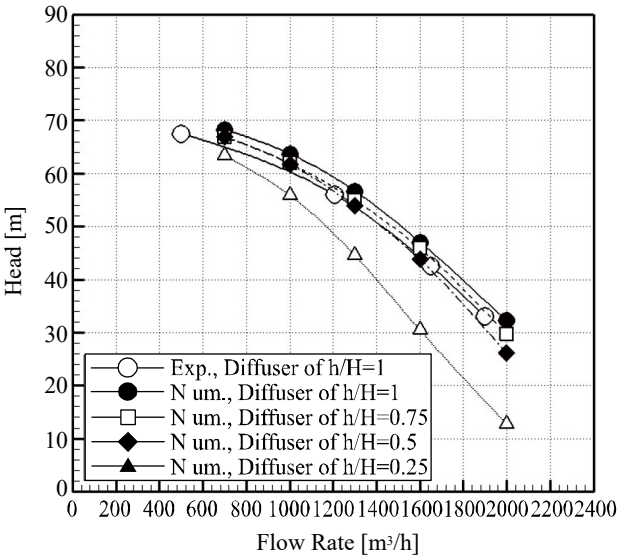


Fig. 6 Variation of head against flow rate for different diffusers

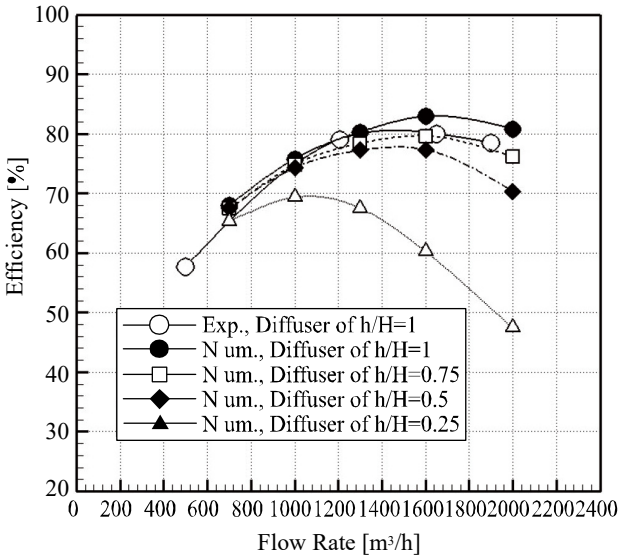


Fig. 7 Variation of overall efficiency against flow rate for different diffusers

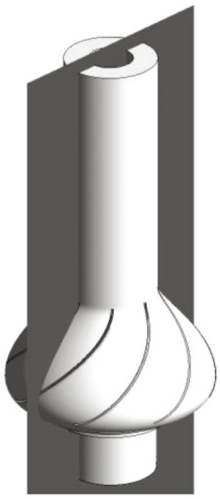


Fig. 8 Mid- plane of the impeller and diffuser

vertically suspended centrifugal pump, computations have been conducted in three dimensions. Indeed, different h/H ratios (h/H= 0.25, 0.5, 0.75 and 1) with vanes leading angle of 10 degree, vanes trailing angle of 90 degree and vanes wrapping angle of 78 degree have been analyzed numerically keeping all other parameters the same and eventually experiments have been performed as cavitation has not been regarded. Besides, the h/H ratio is remained constant at throughout diffuser vane length.

Delivered head values of each investigated diffuser at different flow rates are illustrated in Fig. 6. As it can be seen the diffuser of h/H=1 has the highest head values at all flow rates and the computational data agree well with the experimental results. As pointed out, the highest deviation among them is 8.3 percent. Additionally, the head falls more rapidly by decreasing h/H ratio as the maximum head has been achieved for the diffuser of h/H=1 that is 41.5 percent higher than that of the h/H=0.25 at high flow rate. Fig. 7 indicates the efficiency values of different diffusers against flow rate. There is good compatibility between numerical and experimental results and the computed efficiency at BEP, Best efficiency Point, is 2.9 percent higher than the experimental data. The leakage flow is one reason for differences between numerical and experimental results of delivered head and efficiency. Moreover, ignoring mechanical losses in computations is the other reason associated with these discrepancies. Amongst all surveyed h/H ratios, the highest efficiency values have been obtained for the diffuser of h/H=1 at all flow rates. Actually, in the case of employing not micro-grooved impeller, efficiency of diffuser of h/H=1 is 13.6 percent higher than that of the diffuser of h/H=0.25 at BEP because of the increasing the kinetic energy and the pertinent losses due to the rotational flow field at outlet region of the diffuser with less h/H ratio (h/H=0.25) as shown in subsequent figures. The

https://doi.org/10.1017/jmech.2019.13 Published online by Cambridge University Press

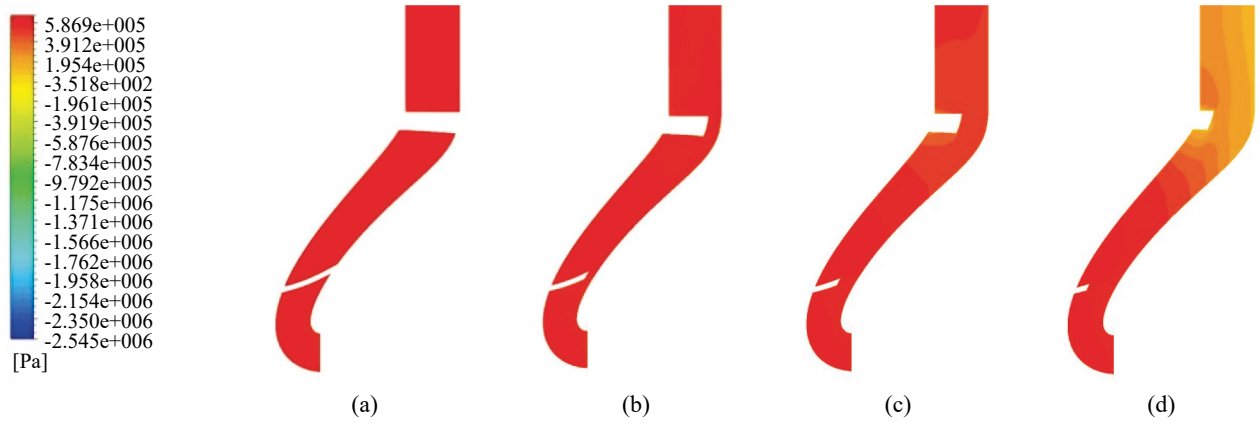


Fig. 9 Pressure distribution (a) Diffuser of h/H=1 (b) Diffuser of h/H=0.75 (c) Diffuser of h/H=0.5 (d) Diffuser of h/H=0.25

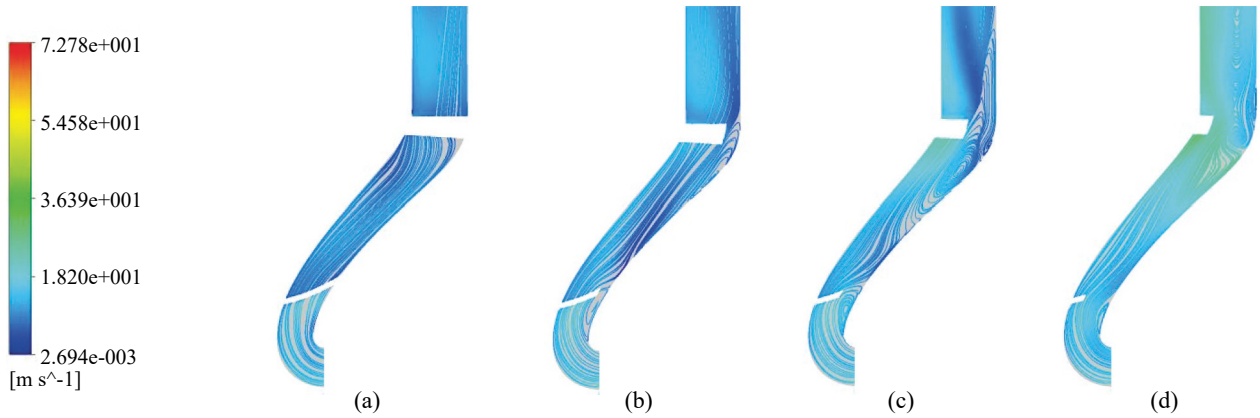


Fig. 10 Velocity streamlines (a) Diffuser of h/H=1 (b) Diffuser of h/H=0.75 (c) Diffuser of h/H=0.5 (d) Diffuser of h/H=0.25

other point is that by reducing h/H ratio, BEP shifts toward the minimum flow rate as the maximum displacement of 30.3 percent has been observed for the diffuser of h/H=0.25 compared to the diffuser of h/H=1.

Fig. 9 depicts pressure distribution of different diffusers at BEP. At the mid- plane of the diffuser, Fig. 8, resulted pressure of the diffusers differ from one another due to the different h/H ratio. Actually, diffuser with h/H=1 has the highest pressure, see Fig. 9 (a), and by declining the h/H ratio, obtained pressure decreases. The reason is that the flow passage area of the diffuser enhances while the rotating flow becomes dominant. Consequently, it provides lower pressure (Figs. 9 (c), (d)).

The flow streamlines of above mentioned diffusers at BEP are given in Fig. 10. Compared other diffusers, diffuser with h/H=1 has more uniform flow field owing to the higher h/H ratio. Some recirculation are created in the diffuser passageways with lower h/H ratio (Figs. 10 (b) and (c)) which are symmetry in the two sides of the diffusers. Moreover, unlike other diffusers with higher h/H ratio there is fewer recirculation in the diffuser of h/H=0.25 (Fig. 10 (d)) since there are rotating flow throughout the diffuser that caused by improper h/H ratio. As a result, the minimum head and efficiency values are resulted in this case.

Fig. 11 presents the streamlines at outlet of all mentioned diffusers with different h/H ratios. The diffusers with lower h/H ratio that encircled the impeller in order to diffuse the high velocity from the impeller circumference have less impact on conversion of kinetic energy to static pressure. Therefore, rotating flow field is resulted at outlet of these diffusers (Figs. 11 (b), (c) and (d)). Whereas, the diffuser of h/H=1 accomplished this diffusion with different passageways that extend from the peripheral impeller to the discharge region of the diffuser. As a result, higher performance is achieved. Moreover, increasing h/H ratio contributes to secondary flow between diffuser passageways and leads to rotating flow decreasing. Figure 11 also shows slightly different flow fields in each section between the diffuser vanes that could convey incoming unsteady flow thru diffuser passageways.

5.2 Influences of leading angle of diffuser vanes

As pointed out previously, in this research, three different vanes leading angles (3, 10 and 17 degree) of a vertically suspended centrifugal pump have been analyzed keeping all other parameters as identical (diffuser vanes with h/H=1, trailing angle of 90 degree and wrapping angle of 78 degree). Performance curves of head and efficiency versus flow rate have been demonstrated in Figs.

https://doi.org/10.1017/jmech.2019.13 Published online by Cambridge University Press

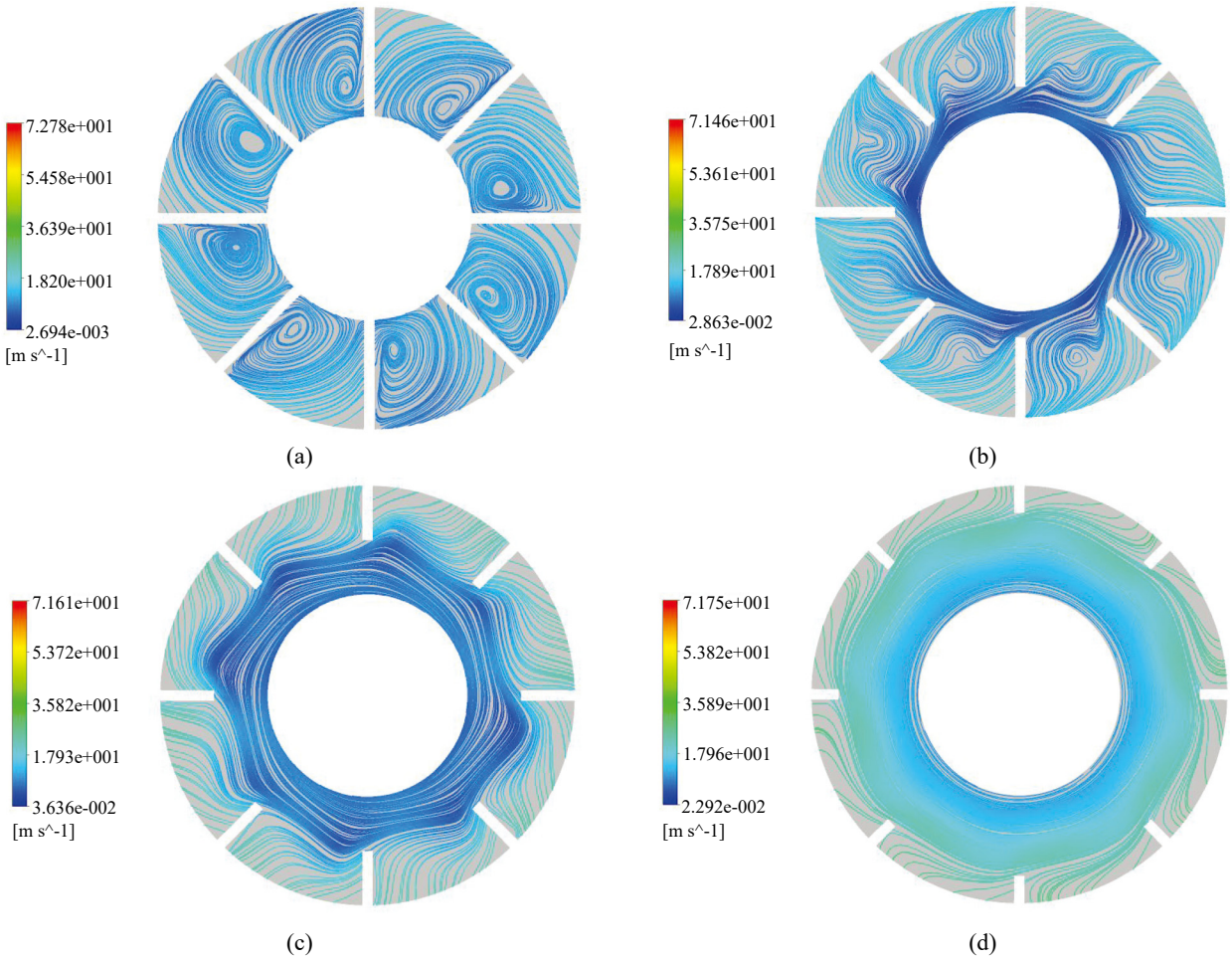


Fig. 11 Flow streamlines (a) Diffuser of h/H=1 (b) Diffuser of h/H=0.75 (c) Diffuser of h/H=0. 5 (d) Diffuser of h/H=0.25

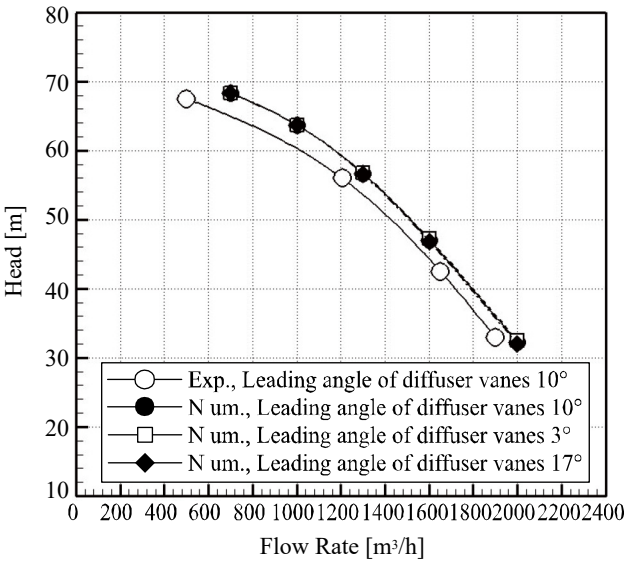


Fig. 12 Variation of head against flow rate for different leading angles of diffuser vanes

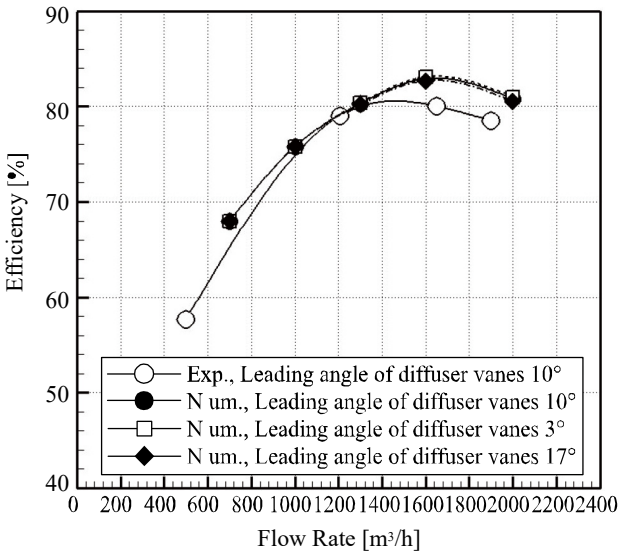


Fig. 13 Variation of overall efficiency against flow rate for different leading angles of diffuser vanes

12 and 13, respectively. According to these figures, making changes of vanes leading angle in the mentioned range has almost no impact on the delivered head of the vertically suspended centrifugal pump as similar outcome was observed by Chung K.N *et al*. [27]. Similarly, efficiency performance of three surveyed diffusers with three different vanes leading angles of 3, 10 and 17 degree remained the same up to BEP but efficiency of the diffuser with vanes leading angle of 3 degree increased negligibly at high flow rate. Whereas, corresponding efficiency of

https://doi.org/10.1017/jmech.2019.13 Published online by Cambridge University Press

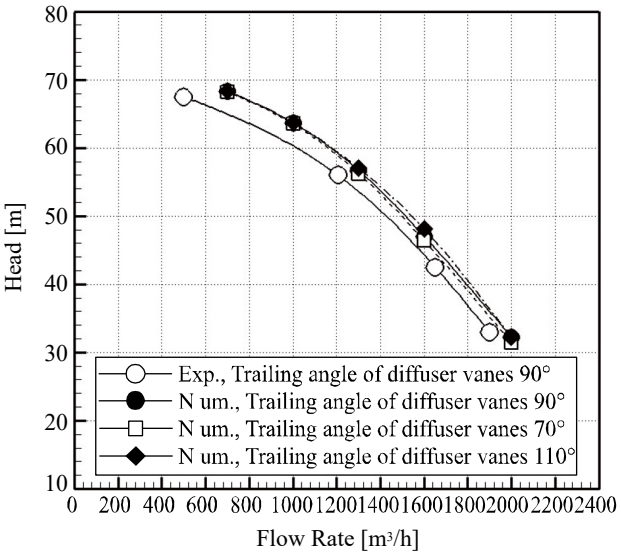


Fig. 14 Variation of head against flow rate for different trailing angles of diffuser vanes

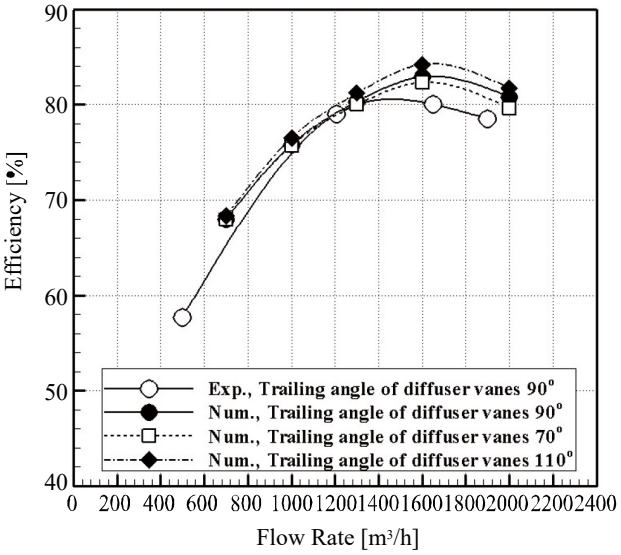


Fig. 15 Variation of overall efficiency against flow rate for different trailing angles of diffuser vanes

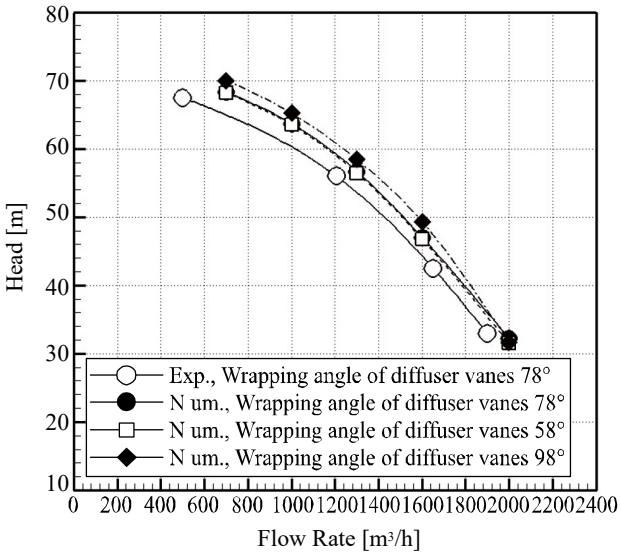


Fig. 16 Variation of head against flow rate for different wrapping angles of diffuser vanes

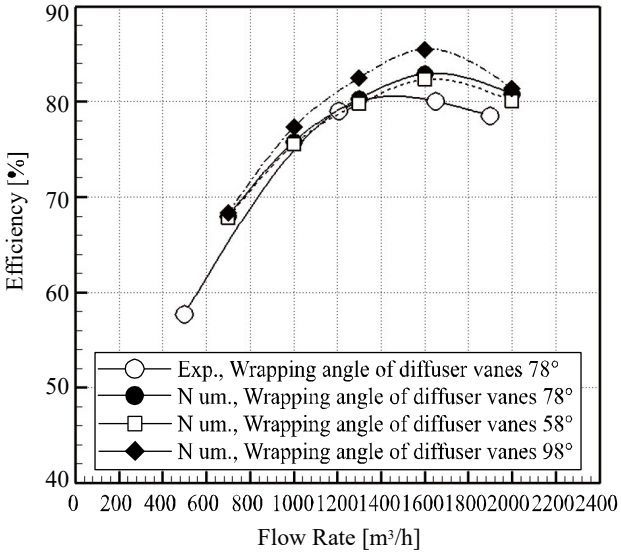


Fig. 17 Variation of overall efficiency against flow rate for different wrapping angles of diffuser vanes

diffuser with vanes leading angle of 17 degree diminished slightly that is consistent with the results of Chung K.N *et al*. [22]. Fig. 13 also depicts differences between BEP position of numerical and experimental results that could be attributed to the mechanical losses and flow in clearances of the tested vertically suspended centrifugal pump.

5.3 Influences of trailing angle of diffuser vanes

Additionally, to study changing impacts of vanes trailing angle on flow characteristics of the vertically suspended centrifugal pump three different trailing angles of 70, 90 and 110 degree have been taken into the account in conditions of former section having vanes leading angle of 10 degree. As illustrated in Figs. 14 and 15, delivered head of all stated cases show almost same trends and values at all flow rates. Meanwhile, increasing flow rate led to some differences for efficiency curves of three aforementioned vanes with different trailing angles as the maximum efficiency has been accomplished using vanes trailing angle 110 degree which is approximately 2 percent higher than that of the 70 degree at BEP owing to better matching between vanes outlet angle and outgoing flow angle.

5.4 Influences of wrapping angle of diffuser vanes

Furthermore, diffuser vanes with different wrapping angles of 58, 78 and 98 degree have also been researched as well. Actually, each investigated case owns the parameters of h/H=1, leading angle of 10 degree and trailing angle of 90 degree equipped with the impeller used in previous sections (not micro grooved impeller).

https://doi.org/10.1017/jmech.2019.13 Published online by Cambridge University Press

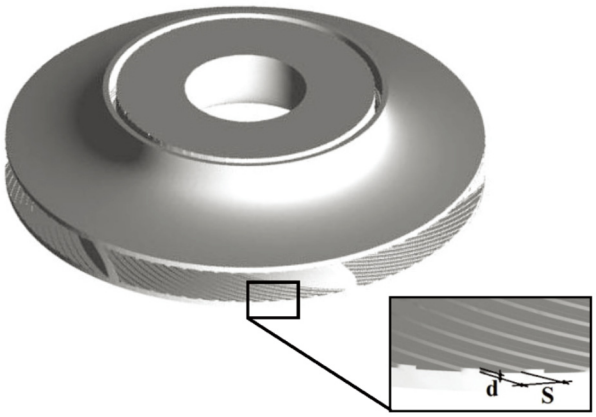


Fig. 18 Isometric view of the micro-grooved impeller with characteristic dimensions of S and d

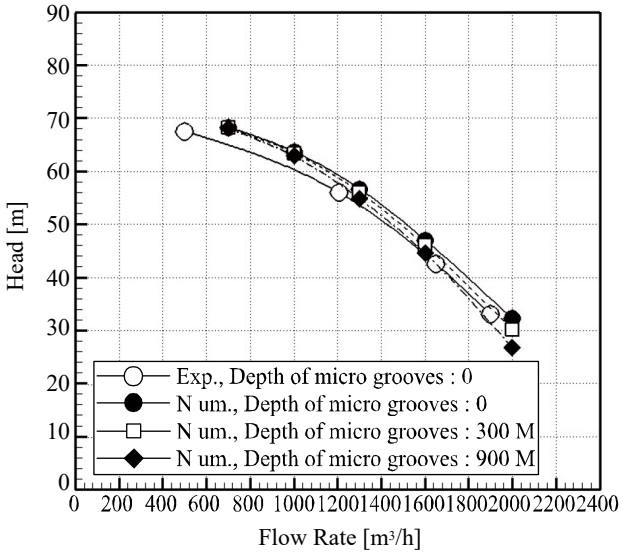


Fig. 19 Variation of head against flow rate for different micro-grooved impellers

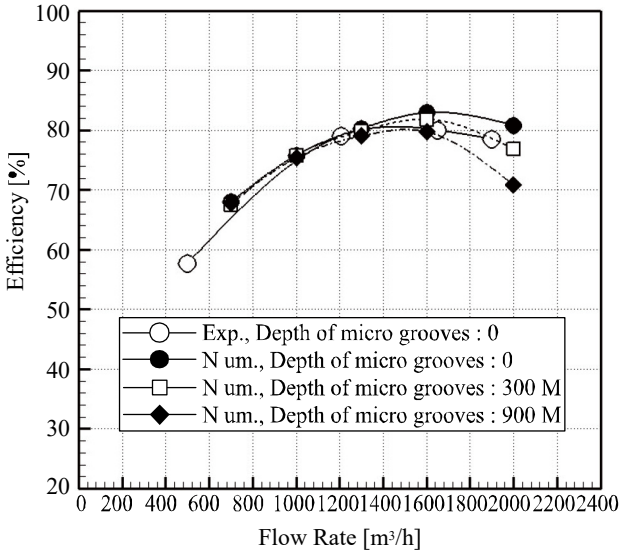


Fig. 20 Variation of overall efficiency against flow rate for different micro-grooved impellers

Figs. 16 and 17 indicate variation of head and efficiency against flow rate for different vanes wrapping angles, respectively. Based on Fig. 16, the highest head value has been accomplished at lowest flow rate for vanes wrapping angle of 98 degree which is 3.5 percent higher than that of two other ones (vanes wrapping angles of 58 and 78 degree). Whereas, due to rising hydraulic losses and skin friction of higher vanes wrapping angle of 98 degree, the related head curve drops more rapidly compared to other vanes wrapping angles as lower head is delivered by the aforementioned diffuser at high flow rate. Likewise, the same behavior of efficiency is seen in Fig. 17 for diffuser with higher wrapping angle (98 degree) at flows higher than that of BEP capacity. Other point is that, in this case, the efficiency of BEP enhanced by 3 percent in comparison with other ones thanks to better conversion of energy within passageways of diffuser associated with higher vanes wrapping angle at BEP.

5.5 Influences of impeller micro grooves depth

In this section, flow characteristics of the vertically suspended centrifugal pump with various depths of impeller micro grooves (0, 300 and 900 micron) in the case of the vaned diffuser of h/H =1, leading angle of 10 degree, trailing angle of 90 degree and wrapping angle of 78 degree have been described. Characteristic dimensions of micro-grooved impellers have been shown in Fig. 18. The results of delivered head and efficiency against flow rate for all investigated impellers have been given in Figs. 19 and 20, respectively. Experimental results for not micro-grooved impeller matched well with numerical data and differences between numerical and experimental results emanating from ignoring gap flow and mechanical losses in computations. By adding micro grooves to the passageways of impeller, unlike the results of Skrzypacz and Bieganowski [11], lower head and efficiency values have been resulted compared to original impeller (d=0 micron). In other word, the more the depth of the micro grooves is the lower the delivered head and efficiency values would be particularly at high flow rate. Indeed, at high flow rate, the micro grooves impacts are more pronounced as there is a maximum head reduction of 16.4 percent for micro-grooved impeller of 900 micron rather than that of the original impeller (d=0 micron). In this case, the corresponding value for micro-grooved impeller of 300 micron was 6.2 percent as well. Indicated pressure and velocity distributions of the micro-grooved and not micro-grooved impellers in Figs. 21 to 22 clarify the reasons for mentioned matter. Also, according to Fig. 20, efficiency of not micro-grooved impeller is higher than that of the micro-grooved impellers at all flow rates. Indeed, increasing depth of micro grooves affects negatively the resulted efficiency values of micro-grooved impellers. Efficiency of micro-grooved impellers also reduce more considerably with flow rate enhancing as efficiency of the impeller with micro grooves of 900 micron is 3.1 percent lower than that of the original impeller (d=0 micron) at BEP. Other point that can be resulted from Fig. 23 is that micro grooves contribute to the position of BEP since the maximum displacement of

https://doi.org/10.1017/jmech.2019.13 Published online by Cambridge University Press



Fig. 21 Pressure distribution (a) Not micro-grooved impeller (b) Micro-grooved impeller (d=300 micron) (c) Micro-grooved impeller (d=900 micron)

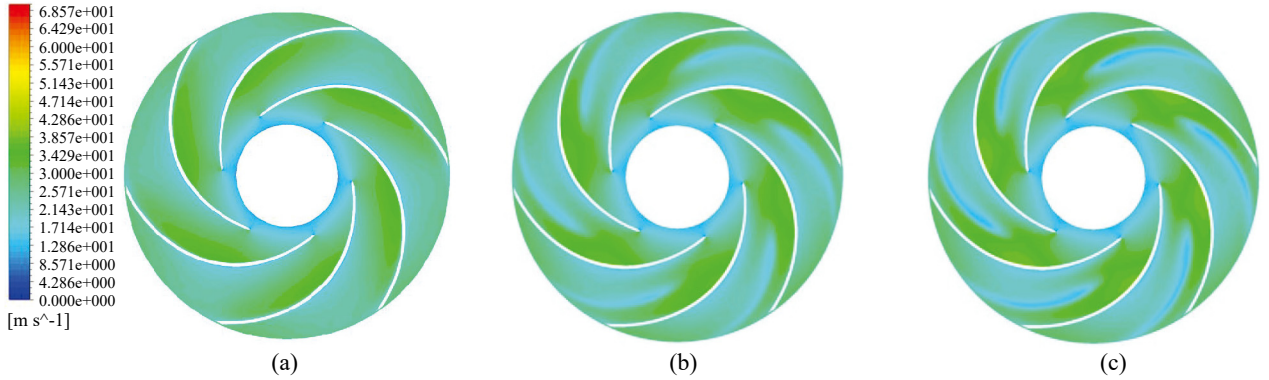


Fig. 22 Velocity distribution (a) Not micro-grooved impeller (b) Micro-grooved impeller (d=300 micron) (c) Micro-grooved impeller (d=900 micron)

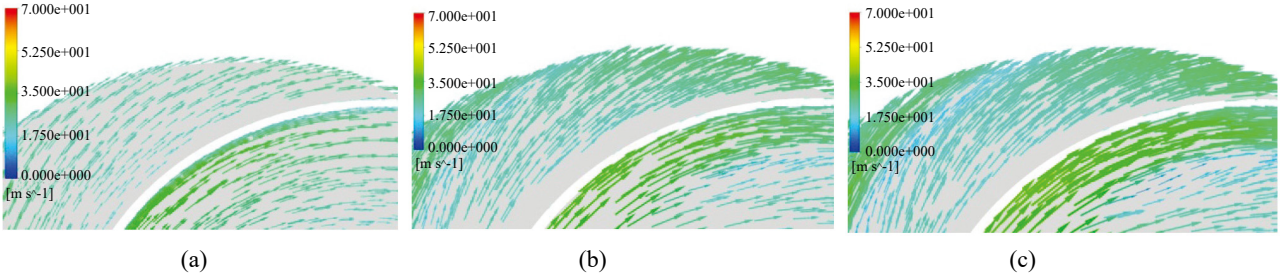


Fig. 23 Velocity vectors (a) Not micro-grooved impeller (b) Micro-grooved impeller (d=300 micron) (c) Micro-grooved impeller (d=900 micron)

BEP has been occurred for micro-grooved impeller of 900 micron which shifted by 6 percent towards the low flow rate. Such a trend has been reported in the Skrzypacz and Bieganowski' studies [11] as well. But, differences of head trend and efficiency trend of the micro-grooved impeller compared to the not micro-grooved impeller resulted in the present research and Skrzypacz and Bieganowski [11] could be due to large difference of pump specific speed. Indeed, the mentioned parameter in the present vertically suspended centrifugal pump is more than twice of that of the pump tested by Skrzypacz and Bieganowski [11]. Consequently, further research are required to study specific speed influences on the performance of centrifugal pumps equipped with micro-grooved impellers.

Distributions of pressure and velocity of micro-grooved and not micro-grooved impellers have been demonstrated in Figs. 21 and 22, respectively. Based on Fig. 21 higher pressure has been obtained in the cross section of not micro-grooved impeller compared to the micro-grooved ones which led to higher head values as stated in the former section. Actually, pressure reduces with the increase of micro grooves depth. Moreover, it is found that micro grooves cause higher dynamic depression in the vicinity of leading edges of blades of micro-grooved impellers in comparison with not micro-grooved impeller. These findings are in accordance with the results from Skrzypacz and Bieganowski [11]. Thus, this phenomenon needs more investigation because impeller micro-grooves might have negative impacts on the cavitation performance of centrifugal pumps. On the contrary, micro grooves lead to higher velocity in micro-grooved impellers (Fig. 22). It can be noticed that by increasing the depth of micro grooves this impact

https://doi.org/10.1017/jmech.2019.13 Published online by Cambridge University Press

becomes stronger (Fig. 22 (c)) thanks to better conduction of flow through passageways of micro-grooved impellers which minimize the probability of recirculating formation. Furthermore, similar to lower velocity of not micro-grooved impeller, lower magnitudes of velocity vectors are seen in middle- span plane of the micro-grooved impeller (Fig. 23 (a)). While, micro-grooved impellers own velocity vectors with higher magnitudes on the impeller circumference and on the passageways (Figs. 23 (b) and (c)). Based on the Fig.23, the highest magnitude of velocity vectors are obtained by the deepest micro-grooved impeller (900 micron).

6. CONCLUSIONS

Influences of different diffuser vanes parameters, h/H=0.25, 0.5, 0.75 and 1 (h is the diffuser vanes height and H is the height of diffuser passage area), leading angles of 3, 10 and 17 degree, trailing angles of 70, 90 and 110 degree, wrapping angles of 58, 78 and 98 degree as well as impeller micro grooves depths, d=0, 300 and 900 micron on the performance of a vertically suspended centrifugal pump, with no cavitation consideration, have been analyzed numerically and then, the optimum case was manufactured to perform experiments (h/H= 1 with leading angles, trailing angles and wrapping angles of 10, 90 and 78 degree, respectively). Numerical results show that h/H ratio of diffuser vanes has the significant effect on the performance of the vertically suspended centrifugal pump followed by the vanes wrapping angle. Increasing the aforementioned angle enhances the efficiency and head more than enhancing the vanes leading and trailing angles. Indeed, by using the diffuser of h/H=1 a head rise of 41.5 percent has been accomplished in comparison with the diffuser of h/H=0.25 at high flow rate. Besides, in this case, the efficiency of BEP climbed by 13.6 percent owing to better conversion of the kinetic energy to static pressure through diffuser passageways of the diffuser of h/H=1. Also, the BEP position is displaced towards the low flow rate by reducing h/H ratio. Furthermore, impeller micro grooves caused more decreasing delivered head and efficiency by flow rate increasing compared to not micro-grooved impeller. Actually, enhancing micro grooves depth resulted in lower pump performance as the maximum difference between head and efficiency of the deepest micro-grooved impeller (900 micron) and not micro-grooved impeller are 16.4 and 3.1 percent, respectively, at high flow rate.

It sounds that more studies could be taken into the account considering specific speed role on the performance of centrifugal pumps equipped with micro-grooved impeller. Also, influences of micro grooves geometries on pump performance and cavitation performance are other issues that need investigations
APPENDIX

NOMENCLATURE

d Depth of a micro groove;
F Source term;
h Diffuser vane height;
H Height of diffuser passage area;
P Pressure;
Ra Arithmetic average of the absolute values of surface roughness, micron;
S Width of a micro groove;
U Velocity;

Eff. Efficiency: $\frac{OutputPower}{InputPower} = \frac{\rho gHQ}{TW}$

T Torque
W Rotating velocity

H Head: $\frac{P(discharge) - P(suction)}{\rho g}$

N_S Specific speed: $\frac{(RPM)(Q[m^3/s])^{0.5}}{(Head[m])^{0.75}}$

Re Reynolds number: $\frac{\rho n D^2}{\mu}$

P Fluid Density;
τ Stress tensor scale;

REFERENCES

1. Zhu J., Zhu H., Zhang J., Zhang H-Q., "A numerical study on flow patterns inside an electrical submersible pump (ESP) and comparison with visualization experiments", *Journal of Petroleum Science and Engineering*, 173, pp. 339-350 (2019).
2. Zhou L., Bai L., Shi W., Li W., Wang C., Ye D., "Numerical analysis and performance experiment of electric submersible pump with different diffuser vanes number", *Journal of the Brazilian Society of Mechanical Sciences and Engineering*, 40 (89) (2018). https://doi.org/10.1007/s40430-018-0986-y
3. Ofuch E.M., Stel H., Vieira T.S., Ponce F.J., Chiva S., Morales R.E.M., "Study of the effect of viscosity on the head and flow rate degradation in different multistage electric submersible pumps using dimensional analysis", *Journal of Petroleum Science and Engineering*, 156, pp. 442-450 (2017).
4. Zhang Q., Xu Y., Cao L., Shi W., Lu W., "A mixed-flow submersible well pump: design features and an investigation of performance", *Journal of the Brazilian Society of Mechanical Sciences and Engineering,* **39**(7), pp. 2561-2569 (2017).
5. Pirouzpanah S., Gudigopuram S. R., Morrison G. L., "Two-phase flow characterization in a split vane impeller Electrical Submersible Pump", *Journal of Petroleum Science and Engineering,* **148**, pp. 82–93 (2017).
6. Zhu J., Banjar H., Xia Z., Zhang H. Q., "CFD simulation and experimental study of oil viscosity effect on multi-stage electrical submersible pump

https://doi.org/10.1017/jmech.2019.13 Published online by Cambridge University Press

(ESP) performance", *Journal of Petroleum Science and Engineering*, **146**, pp. 735–745 (2016).

7. Pineda H., Biazussi J., López F., Oliveira B., Carvalho R. D.M., Bannwart A. C., Ratkovich N., "Phase distribution analysis in an Electrical Submersible Pump (ESP) inlet handling water–air two-phase flow using Computational Fluid Dynamics (CFD)", *Journal of Petroleum Science and Engineering,* **139**, pp. 49–61 (2016).
8. Stel H., Sirino T., Ponce F.J., Chiva S., Morales R.E.M., "Numerical investigation of the flow in a multistage electric submersible pump", *Journal of Petroleum Science and Engineering,* **136**, pp. 41–54 (2015).
9. Zhou L., Shi W., Lu W., Hu B., Wu S., "Numerical investigations and performance experiments of a deep-well centrifugal pump with different diffusers", *ASME Journal of Fluids and Engineering*, **134**(7), pp. 071102 (2012).
10. Sun D., Prado M., "Modeling Gas-Liquid Head Performance of Electrical Submersible Pumps", *Journal of Pressure Vessel Technology*, **127**(1), pp. 31-38 (2005).
11. Skrzypacz J., Bieganowski M., "The influence of micro grooves on the parameters of the centrifugal pump impeller", *International Journal of Mechanical Sciences*, **144**, pp. 827-835 (2018).
12. Khoeini D., Shirani E., "Enhancement of a centrifugal pump performance by simultaneous use of splitter blades and angular impeller diffuser", *International Journal of Fluid Machinery and Systems*, **11** (2), pp. 191-204 (2018).
13. Khoeini D., Shirani E., Joghataei M., "Improvement of centrifugal pump performance by using different impeller diffuser angles with and without vanes", *Journal of Mechanics*, **34**, pp. 1-13 (2018).
14. Khoeini D., Tavakoli M. R., "Flow Characteristics of a Centrifugal Pump with Different Impeller Trimming Methods", *FME Transactions*, **46** (4), pp. 463-468 (2018).
15. Khoeini D., Tavakoli M. R., "The optimum position of impeller splitter blades of a centrifugal pump equipped with vaned diffuser", *FME Transactions*, **46** (2), pp. 205-210 (2018).
16. Chuan W., Weidong S., Xikun W., Xiaoping J., Yang Y., Wei L., Ling Z., "Optimal design of multistage centrifugal pump based on the combined energy loss model and computational fluid dynamics", *Applied Energy*, **187**, pp. 10–26 (2017).
17. Khoeini D., Shirani E., "Influences of Impeller Splitter Blades on the Performance of a Centrifugal Pump with Viscous Fluids", *International Journal of Fluid Machinery and Systems*, **11**(4), , pp. 400-411 (2018).
18. Khoeini D., Riasi A., Shahmoradi A., "Effects of Volute Throat Enlargement and Fluid Viscosity on the Performance of an Over Hung Centrifugal Pump", *International Journal of Fluid Machinery and Systems*, **10** (1), pp. 30-39 (2017).
19. API standard 610, Centrifugal Pumps for Petroleum, Petrochemical and Natural Gas Industries, 10th ed (2004).
20. ISO recommendation R 781, *Measurement of fluid flow by means tubes*. 1st ed. (1968).
21. Moffat, R.J., "Contributions to the theory of single-sample uncertainty" *ASME Journal of Fluids and Engineering*, **104**(2), pp. 250-260 (1982).
22. Barn Menter, F.R., "Two-equation eddy-viscosity turbulence models for engineering applications", *AIAA Journal*, **32**(8), pp. 1598–1605 (1994).
23. Gao, Z. X., Zhu, W. R., Lu, L., Deng, J., Zhang, J. G., Wang, F. J., "Numerical and Experimental Study of Unsteady Flow in a Large Centrifugal Pump With Stay Vanes", *ASME Journal of Fluids and Engineering*, **136** (7), pp. 071101 (2014).
24. Yun R., Zuchao Z., Denghao W., Xiaojun L., "Influence of guide ring on energy loss in a multistage centrifugal pump", *Journal of Fluids Engineering*, **141** (6), pp. 061302 (2018).
25. Zhu X., Li G., Jiang W., Fu L., "Experimental and numerical investigation on application of half vane diffusers for centrifugal pump", *International Communications in Heat and Mass Transfer*, **79**, pp. 114–127 (2016).
26. Fu L., Zhu X., Jiang W., Li G., "Numerical investigation on influence of diffuser vane height of centrifugal pump", *International Communications in Heat and Mass Transfer*, **82**, pp. 114–124 (2017).
27. Chung K. N., Kim J. Y., Park J. H., Kim Y. K., Kim H. C., (2009) A Study of Performance Improvement of Vertical Diffuser Pumps, FEDSM2009-78498.

(Manuscript received August 31, 2018,
accepted for publication March 12, 2019.)

https://doi.org/10.1017/jmech.2019.13 Published online by Cambridge University Press